

Investigation of mechanical and wear behaviour of graphene reinforced aluminium alloy 6061 metal matrix composite

S. Sendhil Kumar¹, S. Dharani Kumar², U. Magarajan^{3*}

¹Department of Mechanical Engineering, Akshaya College of Engineering and Technology, India

²Department of Mechanical Engineering, Sri Eshwar College of Engineering, India

³Department of Mechanical Engineering, Sree Sastha Institute of Engineering and Technology, India

Received 14 October 2019, received in revised form 4 July 2020, accepted 8 July 2020

Abstract

Owing to its outstanding mechanical and thermal properties, graphene has shown enormous potentials as an improvement material for composites. This paper investigates the properties of graphene-reinforced 6061 aluminium alloy Metal Matrix Composites (MMCs) with varying weight percentages (5 and 10 wt.% graphene) of reinforcement. Energy Dispersive Spectroscopy (EDS) and Scanning Electron Microscope (SEM) studies of the MMC confirm the presence and distribution of graphene particles in the Al6061 matrix materials. Mechanical properties such as tensile strength, hardness, and impact strength of MMCs were studied and assessed. Tensile and impact strength of the MMC's increased from 25 to 60 % by the addition of 10 wt.% graphene in aluminium 6061 alloys. The percentage of elongation diminished with the addition of reinforcement in the matrix. The most significant improvement in hardness can be found in additional graphene particles. Wear-test had been performed using the pin-on-disc machine at 10 N load. It was observed that the tribological behaviour of the composite improved after the addition of graphene in Al6061.

Key words: aluminium alloy 6061, graphene, tensile strength, impact strength, voids, debris

1. Introduction

Aircraft, automotive, defence, and transportation industries are in the process of replacing the conventional aluminium alloy material to particle reinforced aluminium alloy composites. For the replacement, scientists, metallurgists, and engineers across the world have been conducting research and development focusing on the aluminium alloy particle reinforced with the Metal Matrix Composite (MMC) for the past decade [1]. One of the essential objectives is to develop an MMC material with a combination of mechanical and wear resistance properties. MMC possesses good mechanical properties, creep and wear-resistance when compared to aluminium alloy [4]. Al6061 is widely used for structural fabrication applications due to its reliable strength, weldability, and corrosion resistance [3]. The heat-treatable 6061 aluminium alloy has replaced the most commonly used matrix alloys of the MMCs [5].

MMCs can be produced by solid state processing, liquid state processing, stir casting, squeeze casting, spray forming, semi-solid forming, and powder metallurgy [3]. Solid state processing provides a desirable mechanical properties, but the investment cost is high [11]. Some of the hard ceramic particles like SiC [12], Al₂O₃ [12], B₄C [15, 17, 19], Si₃N₄ [18] have been mixed with AA6061-based metal matrix using stir casting technique. The optimum amount of reinforcement particles for MMC and carbon-based reinforcement was determined [26].

The effect of flexural strength on graphene Al6061 MMC processed by powder metallurgy was investigated, and its improvement in flexural strength was highlighted as 47 % [26]. Graphene was found to have superior tribological properties even with a minimum usage of 0.3 % [19]; moreover, its additives with lubricant oils [20] reduce the friction. The properties of Al/B₄C nanocomposite were also superior when compared to Al/B₄C micro-composite [15]. A signif-

*Corresponding author: email address: magarajan84@gmail.com

icant increase in elongation of 6061 MMC samples was achieved after adding $\text{Al}_2\text{O}_3/\text{SiC}$ reinforcement nanoparticles [16].

Improvement in the tensile strength and hardness was noticed due to the addition of 6% ZrO_2 and 2% Al6061 MMC [16]. Also, improvement in microhardness value was observed in Al6061 – graphene – SiC MMCs processed by ultrasonic liquid processing [22]. Graphite MMC resulted in the formation of solid lubricant between point-point of a metal surface by reducing the wear loss [18]. Wear-resistance of Al6061 may be successfully improved by the addition of ceramic reinforcements ($\text{Si}_3\text{N}_4 + \text{n-Gr}$) [17].

From the above pieces of literature, it is understood that very few studies have been carried out on the graphene reinforced with Al6061 matrix as MMC composites. Graphene was used as the reinforcement in the experiment discussed in this paper. The primary aim of the presented work is to study the effect of weight percentage of graphene reinforcement in Al6061 alloy and investigate its mechanical and tribological behaviour.

2. Base material and reinforcement

Al6061 is a precipitated and hardened aluminium alloy containing magnesium of 0.8–0.12% and 0.4–0.8% of silicon as its major alloying element and is heat treatable. Thus it has remarkable mechanical and impact properties and also exhibits better weldability and resistance to corrosion.

Graphene has excellent physical, electrical, and mechanical properties such as elastic modulus of 0.5–1 TPa, tensile strength of 130 GPa, thermal conductivity of $5.3 \times 10^3 \text{ W m}^{-1} \text{ K}^{-1}$ and electron mobility of $1500 \text{ cm}^2 \text{ V}^{-1} \text{ s}^{-1}$ and also has an excellent concentration in the field of the composite [18, 19]. Its hardness makes it suitable to be used in defence applications. Graphene proved to be excellent reinforcing material for the MMC [15].

3. Preparation of the composite

In this paper, an aluminium alloy 6061 was used as the matrix material for preparing the metal-matrix composite. Aluminium alloy plate was sliced into small pieces of $10 \times 10 \times 4 \text{ mm}^3$ so that it could be easily placed in graphite crucible for melting. Graphene in powder form was used as the reinforcement. X–Y dimension of graphene approximates to 5–10 μm with an average thickness of 5–10 nm. A molten mixture of matrix and reinforcement were poured into the die and allowed to solidify. The reinforcement particles and matrix were mixed by continuous stirring.

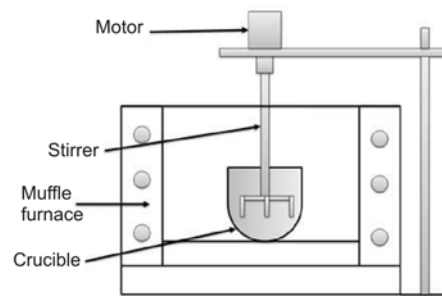


Fig. 1. Schematic diagram of the stir casting setup used for making the samples.

Figure 1 shows the stir casting machine used for the production of MMC.

Al6061 sliced plate was kept inside a coated graphite crucible. Initially, the sliced plate was preheated for 2 h at 450°C in a muffle furnace, to remove the surface oxides. The furnace temperature was raised above the liquid temperature of aluminium alloy (750°C) to melt the aluminium alloy completely.

The graphene powder was mechanically mixed below its melting point, and 1 wt.% of magnesium powder was added. Addition of the magnesium reduces the surface tension, thereby enhancing the usability of aluminium melt. Stirring of the material was executed for 10 min with a speed of 290 rpm at 750°C . To obtain the uniform distribution, angle of 60° was provided in the stirring blade. The proper stirring produced the best mixing results in a uniform microstructure compared to a conventional stirring. Preheating of the moulds was performed at $250\text{--}350^\circ\text{C}$ for 2 h before pouring the melt. After the removal of slag, the composite melt was transferred to the preheated mould.

This procedure was repeatedly done by varying the composition percentage of the reinforcement powder. For each composition, 500 g of Al6061 matrix material was used for preparing the samples along with 1 wt.% Mg. After solidification, the casting and the samples were removed from the mould. The samples are shown in Figs. 2a,b. Three samples were prepared, sample A contains AA6061 with 1 wt.% Mg, sample B contains 5 wt.% graphene, and sample C contains 10 wt.% graphene.

4. Confirmation of the composition

To confirm the distribution of graphene in the Al6061 MMC, EDS analysis was performed. Figures 3a,b illustrate the spectrum of the EDS analysis of sample B and sample C composites. Each peak corresponds to the presence of an element in the MMC. From the spectrum, it is inferred that the largest peak



Fig. 2. Cast samples of MMCs.

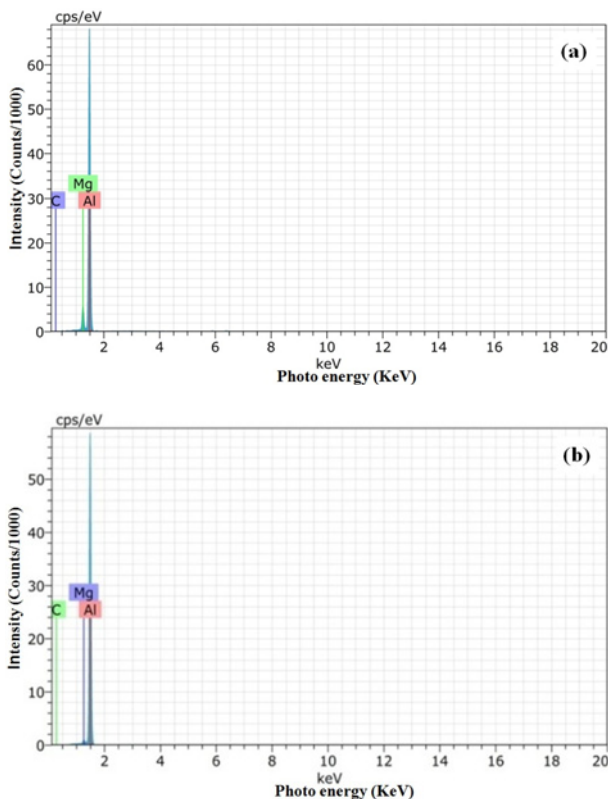


Fig. 3. Image of graphene reinforced MMC: (a) EDS sample B and (b) EDS sample C.

corresponds to aluminium as it is the matrix material present in MMC. Adjacent to aluminium is the peak that corresponds to graphene and magnesium, which are also presented in MMC. SEM image in Fig. 3b shows the existence of graphene particles in Al6061 with 10 wt.% graphene MMC sample C. It can be thus noticed that the graphene particles are dispersed into

the Al6061 matrix. EDS images of both MMC samples show there is no significant presence of alumina, magnesia, and silicon carbide. This can be attributed to the fact that the presence of magnesium and silicon is very negligible. Also, the oxides of alumina will be removed as slag during the stir casting process.

5. Testing

The following mechanical tests were conducted on the Al6061 composites to determine their mechanical properties.

5.1. Tensile test

The ability of a material to resist a static load can be determined by a tensile test of the material. The tensile test is used in evaluating the fundamental properties such as yield strength, ultimate tensile strength, and percentage of elongation of the developed composite material. Tensile strength of AA6061 and MMC samples was evaluated using UTM machine as per the ASTM E8-M04. The tensile test specimen was machined as per ASTM: B-557 standard. A tensile test was performed using electron mechanical controlled Instron UTM with an ultimate load of 100 kN.

5.2. Hardness test

The hardness test is used to evaluate the resistance of a material to permanent deformation when a force is applied. The Brinell hardness test is carried out to determine the magnitude of the hardness of metal matrix composite. Hardness test was carried out according to the ASTM E10 standards using 10 mm steel ball indenter of 500 Kgf load.

5.3. Impact test

Charpy impact testing of materials involves a dynamic application of the load before failure. This test measures the toughness value of the material. The specimen was prepared as per ASTM E23-04 standard.

5.4. Wear test

The wear experiment was carried out according to ASTM G 99-95 standards using a pin on disc testing machine (DUCOM, INDIA) with disc material of specifications: EN 32 steel (hardness: 62 HRC). Pin on disc apparatus is shown in Fig. 4. The machine consists of a pin holder connected with the loading lever and LVDT to measure the wear loss. The stir cast specimens were machined in the form of pins with the diameter of 10 mm and height of 25 mm and were

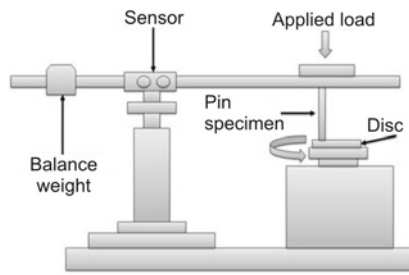


Fig. 4. Schematic diagram of the pin on disc apparatus used for testing the wear behaviour of samples.

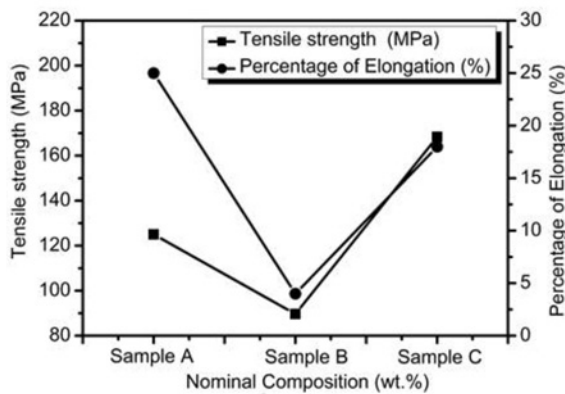


Fig. 5. Tensile test plot of samples A, B, and C.

tested against a rotating disk. The wear test was conducted by applying a load of 10 N along with sliding speed of 1.0 m s^{-1} at a distance of 2000 m at room temperature. During sliding, the load was applied to the specimen, and it was brought into intimate contact with the rotating disc [12]. Wear loss was evaluated by measuring the weight of samples before and after the test.

6. Results and discussion

Composite was subjected to various tests to determine its material properties. Based on the testing of the composites, the following results are observed.

6.1. Tensile test results

Figure 5 shows the comparison of tensile strength and percentage of elongation for the three samples. It was found that sample C has a higher tensile strength of 168.33 MPa than the other samples. But the % of elongation is lower than that for the samples A and B. Addition of 5 wt.% graphene declines the tensile strength compared to that for sample C. This is due to the insufficient amount of reinforcement particles,

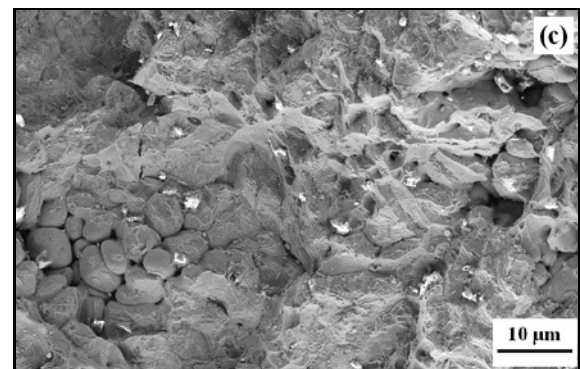
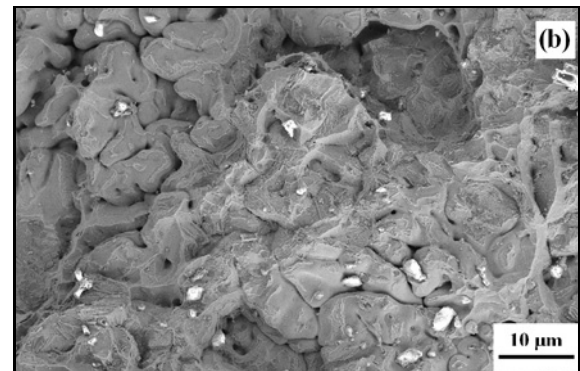
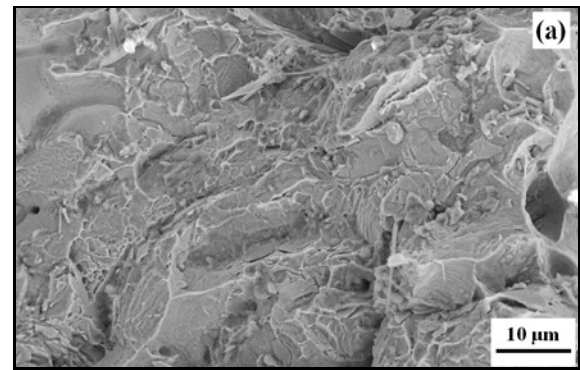


Fig. 6. Fractured SEM images after tensile testing of samples A, B, and C.

which causes improper interfaces in MMC and leads to quick crack initiation. Tensile failure in the composite is controlled by the progressive fracture of reinforcement particles [8]. Figures 6a–c depict the SEM images of fractured samples after the conduct of the tensile test.

Sample A (25 % of elongation) has a higher percentage of elongation than the sample B (4 % of elongation) and sample C (18 % of elongation) due to the addition of the reinforcement particles which reduces ductility. As the percentage of reinforcement particles increases, a reduction in ductility was observed [1, 6, 23]. Increase in reinforcement particles resulted in a better interface and good matrix bonding, which may be due to the reason for sample C to possess good

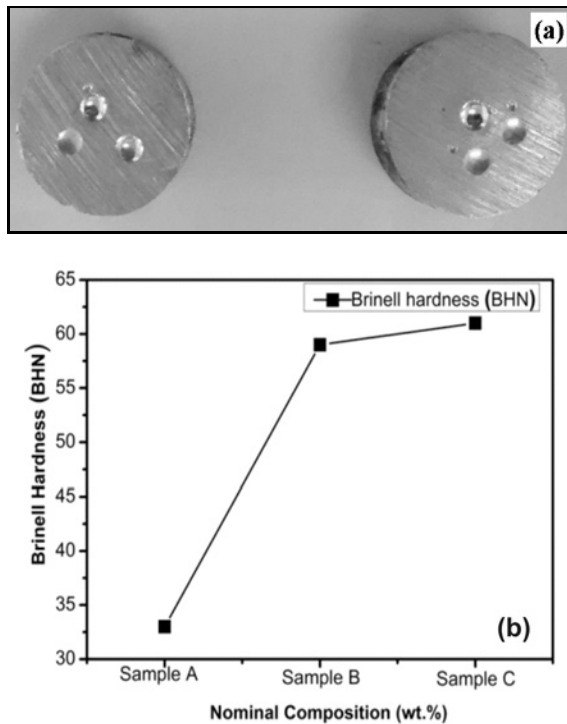


Fig. 7. (a) Brinell hardness test samples and (b) hardness graph of samples A, B, and C.

tensile properties. Similar tensile results are observed in [13, 14]. However, the tensile results of the present study are comparable with the previous work [25] for the same alloy Al6061 but for different reinforcements. Tensile strength reported in [25] was 128.24 MPa and its 23 % inferior to sample C of the presented study.

6.2. Hardness test

Brinell hardness test was carried out for the samples, and the tested samples are shown in Fig. 7a. Figure 7b shows the plot of Brinell hardness for different samples. From the graph, it is observed that there was a better enhancement in the hardness value with the addition of reinforcement. It has been noted that the hardness value of sample C is 3.27 % higher than that of sample B. This is due to the presence of a high amount of reinforced graphene particles. In short, the addition of reinforcement particles in the matrix increases the hardness [1, 6, 8]. Lower accumulation of graphene may cause more slippage between graphene flakes, which will affect the grain growth. Addition of more reinforcement particles acts as a grain development inhibitor leading to the formation of fine grains that improves the hardness. However, the process fills the voids at lesser content [17]. Hence, the graphene reinforcement particles significantly improves the hardness.

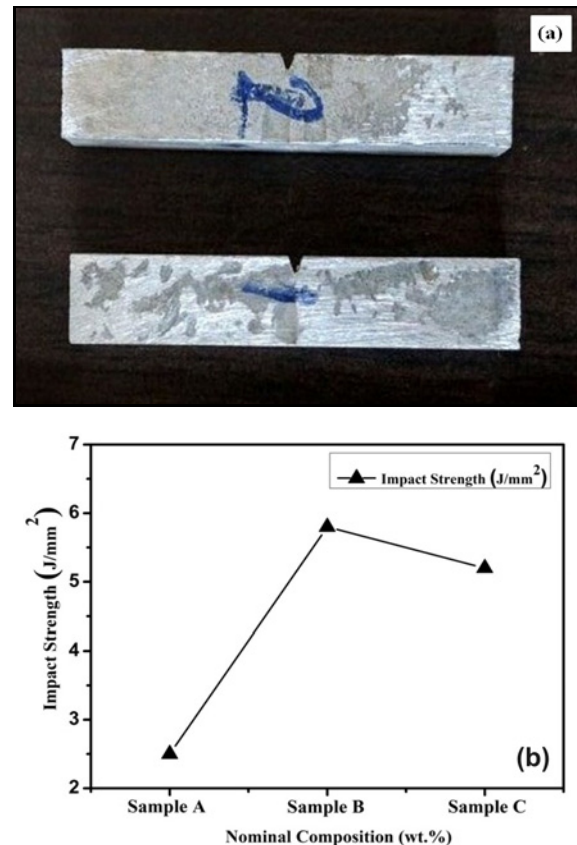


Fig. 8. (a) Sample prepared for impact test and (b) impact test result of samples A, B, and C.

6.3. Impact test

Charpy impact test was performed as per the ASTM E23-04 with V-notched specimen, as shown in Fig. 8a. The observed impact strength of three different samples is shown in Fig. 8b. It can be noticed that sample B has got superior impact strength compared to other samples. Sample B contains the least amount of graphene, which makes it ductile, hence absorbing more impact energy.

Moreover, 1.21 % of the decrease in the impact strength was noticed when increasing the reinforcement particles. The primary reason for the reduction in the impact strength of sample C is due to the presence of carbides. Hence, it increases the hardness and reduces the impact strength. A similar result was noticed in the work of in-situ TiAl composites: where the volume fraction of carbides increases, there is a decrease in the impact strength [27]. The least amount of SiC with 0.5 wt.% reinforcement [26] in Al6061 absorbs more impact energy when compared to 1 and 2 wt.% SiC. However, with a minimum increment of graphene considerably changes the impact strength. The increase in impact strength of MMC, when compared with pure Al6061 alloy, is 50 %.

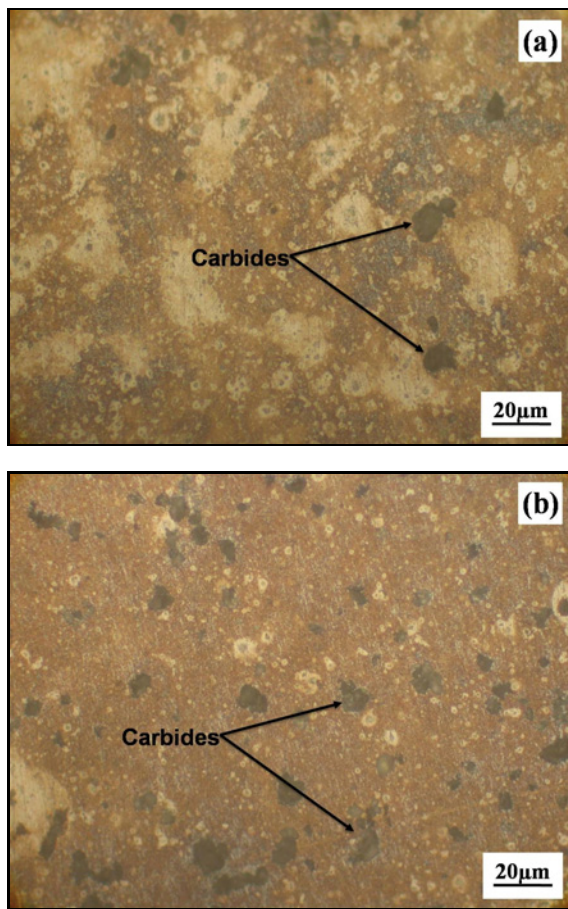


Fig. 9. Optical microstructure of MMC: (a) sample B and (b) sample C.

6.4. Effect of carbide on mechanical properties

The microstructures of aluminium metal matrix composites of sample B and sample C are shown in Figs. 9a,b. Both the microstructures clearly indicate the presence of carbide inclusions in the aluminium matrix. However, predominantly more carbides are noticed in sample C compared with sample B.

The addition of graphene was higher in sample C compared to sample B. Figures 10a,b represent the higher magnification SEM microstructure of sample B and sample C. SEM images clearly indicate the presence of graphene and carbides. The white regions are graphene, and the black areas are carbides. The amount of carbide formation in sample C is higher than in sample B, because of the higher percentage of graphene particles.

The finely dispersed carbide particles may be the reason for an increase in the strength and hardness of MMC. Very few amounts of carbide in the aluminium metal matrix would increase the strength of the composite [29]. However, a decrease in ductility was noticed in MMC, which may be due to the accu-

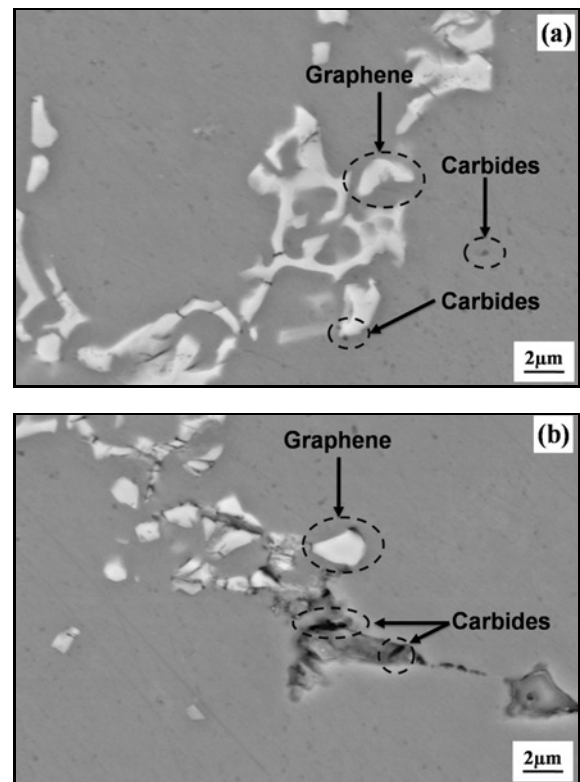


Fig. 10. SEM microstructure of MMC: (a) sample B and (b) sample C.

mulation of carbide particles, thus reducing the elastic deformation and increasing the strength of MMC. The higher wt.% of graphene in the MMCs results in an increase of carbides. Therefore, the strength and hardness of composite are increased. However, there is a decrease in the impact strength and wear resistance which may be due to a higher concentration of carbides for 10 wt.% of graphene composite.

6.5. Wear test

Pin samples A, B, and C were cast with a diameter of 10 mm and length of 40 mm for all of them as shown in Figs. 11a–c. The surface of all samples was well cleaned with acetone and polished with different grades (400 and 600 μm) of abrasive papers. Figure 12 shows the variation in the wear (in microns) of different samples with a constant sliding time of 10 min. Wear in microns for each sample was calculated, based on the normal force and the frictional force between the pin and rotating disc. It was observed that sample B possessed the least wear of 58 microns compared to sample C (86 microns) and A (119.87 microns). It is much easier to have graphene in mechanically mixed layers during friction when compared to sample C with higher carbide concentration. A decrease in the material hardness was observed in sample B, which consists

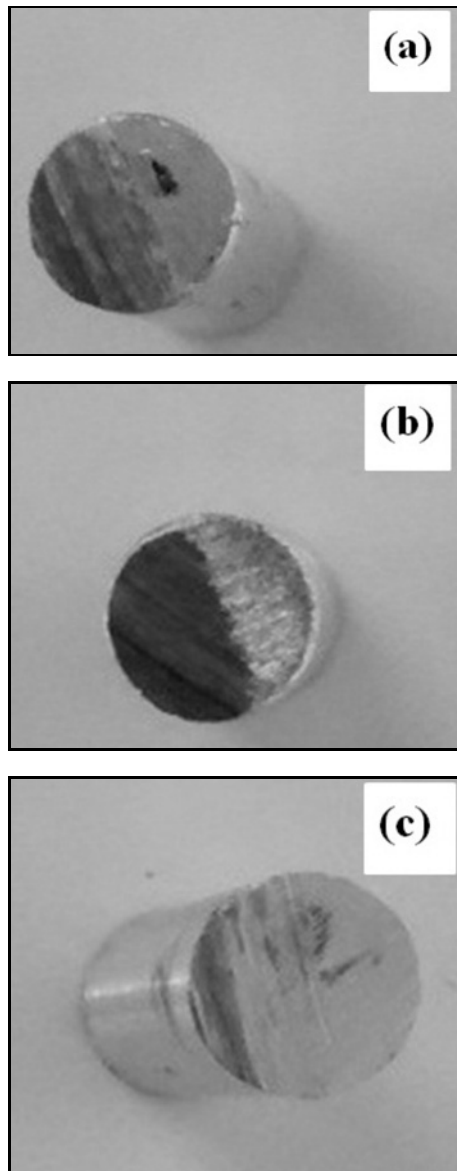


Fig. 11. Samples used for wear testing.

5 wt.% graphene. During wear test of the frictional heat was generated, and as a result, the graphene became lubricant and makes the MMC's more ductile. It can be concluded from the study that higher percentages of graphene content significantly reduce the wear loss of Al6061 MMC's [15]. The graphene reinforcement was significant in this study, and it decreased the wear of MMC when observed for about 2 h.

6.6. Microstructural study of wear samples

Figures 13a–c illustrate the worn surfaces and wear debris of test samples examined through SEM. The abrasion induced plastic damage and grooves along sliding direction on the worn surface of Al6061, as

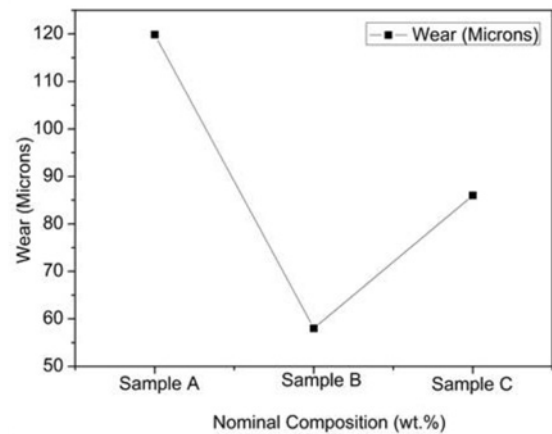


Fig. 12. Comparative graph for wear test results of samples A, B, and C.

shown in Fig. 13a. The worn surface of sample A has undergone severe plastic deformation since it does not contain graphene that makes the ductile for more debris and cross-hatching lines, whereas sample B, as shown in Fig. 13b, possessed the batch of the plug off formed due to the lesser percentage of reinforcement particles, and a crack was also observed. This may cause improper interfaces in MMC and lead to crack propagation. These cracks led to the formation of delimitation debris. Plug off and cracks were less when the percentage of graphene decreased. Figure 13c indicates that the worn surface of sample C possessed a few micro-cracks and wear debris when compared to sample A and B. The samples without reinforcement content show more defects compared to Al6061 graphene composites, which were tested under constant load and time. Hence, the wear damage behaviour of the Al6061 was reduced by fabricating the MMC using 10 wt.% graphene.

7. Conclusions

In this paper, Al6061-graphene composites of different weight percentage (5 and 10 wt.% graphene) were fabricated using stir casting technique. EDS and SEM observations confirmed the presence of graphene, mixed adequately with Al6061 base metal during stir casting.

The tensile strength of the Al6061 was improved by the addition of 10 wt.% graphene reinforcement particles, which was 25 % superior to unreinforced Al6061. Addition of graphene particles decreased the ductility and improved the load-carrying capacity.

It was observed that the hardness of sample C was higher than of other samples. The effect of a small amount of graphene particles marginally improved the hardness properties. It was also noted that the impact

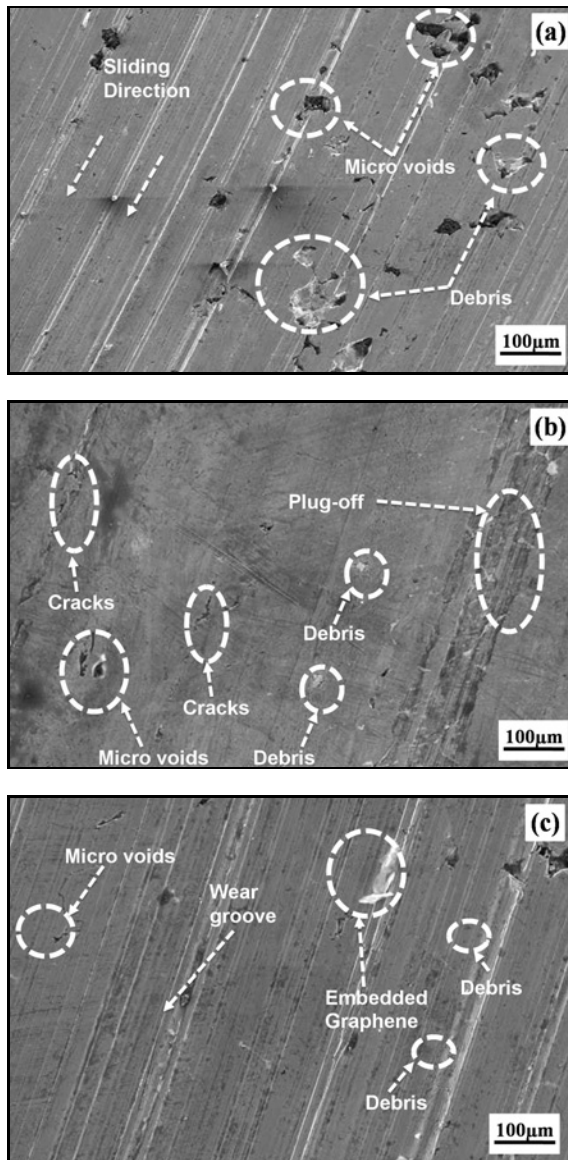


Fig. 13. SEM images of the wear samples A, B, and C.

strength of composites Al6061 increased by the addition of graphene reinforcement particles. The maximum impact strength of 6.138 Jmm^{-2} was found in 5 wt.% graphene composite. However, in 10 wt.% graphene composite, there seems a 6 % reduction in impact strength when compared with 5 wt.% graphene composite. The addition of graphene reinforcement particles in the Al6061 improved the strength, hardness, and reduced the ductility and impact strength.

The wear results showed that sample B (58 microns) has the least wear rate when compared to the other two samples. SEM observation showed that the plug off and debris analysis of MMC confirmed the insufficient presence of graphene and Al6061 base metal had more wear damage surfaces. This greatly influenced the effect of wear when compared to graphene

reinforcement samples. It can be concluded that 5 wt.% graphene MMC can be considered as a suitable material for various structural and wear applications.

To conclude, strength and hardness increase with the presence of carbides in the composite. However, there is a decrease in impact and wear properties which may be due to a higher concentration of carbides. Hence the formation of carbides will act as strong and innocuous effect on the mechanical properties. Therefore, the effects of the addition of the different weight percentage of graphene reinforcement in the aluminium matrix were investigated.

References

- [1] J. Corrochano, C. Cerecedo, V. Valcárcel, M. Lieblich, F. Guitián, Whiskers of Al_2O_3 as reinforcement of a powder metallurgical 6061 aluminium matrix composite, *Materials Letters* 62 (2008) 103–105. [doi:10.1016/j.matlet.2007.04.080](https://doi.org/10.1016/j.matlet.2007.04.080)
- [2] J. Johny James, K. Venkatesan, P. Kuppan, R. Ramanujam, Hybrid aluminium metal matrix composite reinforced with SiC, *Procedia Eng.* 97 (2014) 1018–1026. [doi:10.1016/j.proeng.2014.12.379](https://doi.org/10.1016/j.proeng.2014.12.379)
- [3] K. J. Lijay, J. D. R. Selvam, I. Dinaharan, S. J. Vijay, Microstructure and mechanical properties characterization of AA6061/TiC aluminum matrix composites synthesized by in situ reaction of silicon carbide and potassium fluotitanate, *Trans. Nonferrous Met. Soc. China* 26 (2016) 1791–1800. [doi:10.1016/S1003-6326\(16\)64255-3](https://doi.org/10.1016/S1003-6326(16)64255-3)
- [4] B. N. Sarada, P. L. S. Murthy, G. Ugrasen, Hardness and wear characteristics of hybrid aluminium metal matrix composites produced by stir casting technique, *Mater. Today Proc.* 2 (2015) 2878–2885. [doi:10.1016/j.matpr.2015.07.305](https://doi.org/10.1016/j.matpr.2015.07.305)
- [5] C. Dubey, Corrosion behaviour of TiB_2 reinforced aluminium based in situ metal matrix composites, *Perspect. Sci.* 8 (2016) 172–175. [doi:10.1016/j.pisc.2016.04.025](https://doi.org/10.1016/j.pisc.2016.04.025)
- [6] A. J. Knowles, X. Jiang, M. Galano, F. Audebert, Microstructure and mechanical properties of 6061Al alloy based composites with SiC nanoparticles, *J. Alloys Compd.* 615 (2014) 401–405. [doi:10.1016/j.jallcom.2014.01.134](https://doi.org/10.1016/j.jallcom.2014.01.134)
- [7] Y. Li, K. T. Ramesh, E. S. C. Chin, Comparison of the plastic deformation and failure of A359/SiC and 6061-T6/ Al_2O_3 metal matrix composites under dynamic tension, *Materials Science and Engineering A* 371 (2004) 359–370. [doi:10.1016/j.msea.2004.01.008](https://doi.org/10.1016/j.msea.2004.01.008)
- [8] B. V. Ramnath, C. Elanchezian, M. Jaivignesh, S. Rajesh, C. Parswajinan, A. S. Ahmed, Evaluation of mechanical properties of aluminium alloy-alumina-boron carbide metal matrix composites, *J. Mater.* 58 (2014) 332–338. [doi:10.1016/j.matdes.2014.01.068](https://doi.org/10.1016/j.matdes.2014.01.068)
- [9] R. Ambigai, S. Prabhu, Experimental and ANOVA analysis on tribological behavior of Al/ B_4C micro and nanocomposite, *Aust. J. Mech. Eng.* 486 (2017) 53–63. [doi:10.1080/14484846.2017.1299663](https://doi.org/10.1080/14484846.2017.1299663)
- [10] J. L. Li, S. S. Li, Y. C. Xiong, Nanostructured powder for nano- B_4C particulate-reinforced aluminium-matrix composite prepared via cryomilling, *Materials*

- Research Innovations 19 (2015) 148–152. [doi:10.1179/1432891715Z.0000000001948](https://doi.org/10.1179/1432891715Z.0000000001948)
- [11] P. Taylor, J. Ye, B. Q. Han, J. M. Schoenung, Mechanical behavior of an Al-matrix composite reinforced with nanocrystalline Al-coated B₄C particulates, *Philosophical Magazine Letters* 86 (2015) 37–41. [doi:10.1080/09500830600986109](https://doi.org/10.1080/09500830600986109)
- [12] N. Sharma, R. Khanna, G. Singh, V. Kumar, Fabrication of 6061 aluminium alloy reinforced with Si₃N₄/N-Gr and its wear performance optimization using integrated RSM-GA, *Particulate Science and Technology* 6351 (2016) 731–741. [doi:10.1080/02726351.2016.1196276](https://doi.org/10.1080/02726351.2016.1196276)
- [13] S. Jia, Y. Xuan, L. Nastac, Paul G. Allison, T. W. Rushing, Microstructure, mechanical properties and fracture behavior of 6061 aluminium alloy-based nano composite castings fabricated by ultrasonic processing, *International Journal of Cast Metals Research* 461 (2016) 286–289. [doi:10.1080/13640461.2016.1181232](https://doi.org/10.1080/13640461.2016.1181232)
- [14] Y. Chen, T. Chen, S. Zhang, P. Li, Effects of processing parameters on microstructure and mechanical properties of powder-thixoforged 6061 aluminum alloy, *Trans. Nonferrous Met. Soc. China* 25 (2015) 699–712. [doi:10.1016/S1003-6326\(15\)63655-X](https://doi.org/10.1016/S1003-6326(15)63655-X)
- [15] H. G. Prashantha Kumar, M. A. Xavier, Effect of graphene addition and tribological performance of Al 6061/graphene flake composite, *Tribol. Mater. Surf. Interfaces* 11 (2017) 1–10. [doi:10.1080/17515831.2017.1329920](https://doi.org/10.1080/17515831.2017.1329920)
- [16] R. Pandiyarajan, P. Maran, S. Marimuthu, K. C. Ganesh, Mechanical and tribological behavior of the metal matrix composite AA6061/ZrO₂, *Journal of Mechanical Science and Technology* 31 (2017) 4711–4717. [doi:10.1007/s12206-017-0917-3](https://doi.org/10.1007/s12206-017-0917-3)
- [17] S. Vijayakumar, L. Karunamoorthy, Modelling and analysis on wear behaviour of aluminium metal matrix composites: A statistical approach, *Tribol. Mater. Surf. Interfaces* 5 (2011) 65–71. [doi:10.1179/1751584X11Y.0000000007](https://doi.org/10.1179/1751584X11Y.0000000007)
- [18] A. Baradeswaran, A. Elayaperumal, Mechanical and tribological behaviour of graphite-reinforced aluminium matrix composites, *Journal of the Balkan Tribological Association* 19 (2013) 354–364.
- [19] J. Lin, L. Wang, G. Chen, Modification of graphene platelets and their tribological properties as a lubricant additive, *Tribol. Lett.* 41 (2011) 209–215. [doi:10.1007/s11249-010-9702-5](https://doi.org/10.1007/s11249-010-9702-5)
- [20] K. Shibata, T. Yamaguchi, T. Urabe, Experimental study on microscopic wear mechanism of copper/carbon/ rice bran ceramics composites, *Wear* 294 (2012) 270–276. [doi:10.1016/j.wear.2012.07.004](https://doi.org/10.1016/j.wear.2012.07.004)
- [21] M. Bastwros, G.-Y. Kim, C. Zhu, K. Zhang, S. Wang, X. Tang, X. Wang, Effect of ball milling on graphene reinforced Al6061 composite fabricated by semi-solid sintering, *Composites Part B* 60 (2014) 111–118. [doi:10.1016/j.compositesb.2013.12.043](https://doi.org/10.1016/j.compositesb.2013.12.043)
- [22] S. Jauhari, H. G. Prashantha Kumar, M. A. Xavier, Synthesis and characterization of AA 6061-graphene-SiC hybrid nanocomposites processed through microwave sintering, *IOP Conference Series: Materials Science and Engineering* 149 (2016) 1–6. [doi:10.1088/1757-899X/149/1/012086](https://doi.org/10.1088/1757-899X/149/1/012086)
- [23] V. Umasankar, Experimental evaluation of the influence of processing parameters on the mechanical properties of SiC particle reinforced AA6061 aluminium alloy matrix composite by powder processing, *J. Alloys Compd.* 582 (2014) 380–386. [doi:10.1016/j.jallcom.2013.07.129](https://doi.org/10.1016/j.jallcom.2013.07.129)
- [24] S. Rajakumar, C. Muralidharan, V. Balasubramanian, Establishing empirical relationships to predict grain size and tensile strength of friction stir welded AA 6061-T6 aluminium alloy joints, *Trans. Nonferrous Met. Soc. China* 20 (2010) 1863–1872. [doi:10.1016/S1003-6326\(09\)60387-3](https://doi.org/10.1016/S1003-6326(09)60387-3)
- [25] P. Subramanya Reddy, R. Kesavan, B. Vijaya Ramnath, Investigation of mechanical properties of aluminium 6061-silicon carbide, boron carbide metal matrix composite, *Silicon* 10 (2018) 495–502. [doi:10.1007/s12633-016-9479-8](https://doi.org/10.1007/s12633-016-9479-8)
- [26] H. G. Prashantha Jauhari, M. A. Xavier, Processing and characterization of Al 6061-graphene nanocomposites, *Materials Today: Proceedings* 4 (2017) 3308–3314. [doi:10.1016/j.matpr.2017.02.217](https://doi.org/10.1016/j.matpr.2017.02.217)
- [27] J. Lapin, A. Klimová, Z. Gabalcová, T. Pelachová, O. Bajana, M. Štamborská, Microstructure and mechanical properties of cast in-situ TiAl matrix composites reinforced with (Ti, Nb)₂AlC particle, *Material and Design* 133 (2017) 404–415. [doi:10.1016/j.matdes.2017.08.012](https://doi.org/10.1016/j.matdes.2017.08.012)
- [28] A. Klimová, J. Lapin, Effect of Al content on microstructure of Ti-Al-Nb-C-Mo composites reinforced with carbide particles, *Kovove Mater.* 57 (2019) 377–387. [doi:10.4149/km_2019_6_377](https://doi.org/10.4149/km_2019_6_377)
- [29] S. F. Bartolucci, Joseph Paras, M. A. Rafiee, J. Rafiee, S. Lee, D. Kapoor, N. Koratkar, Graphene-aluminum nanocomposites, *Mater. Sci. Eng. A* 27 (2011) 7933–7937. [doi:10.1016/j.msea.2011.07.043](https://doi.org/10.1016/j.msea.2011.07.043)
- [30] W. Strunk Jr., E. B. White, *The Elements of Style*, fourth ed., Longman, New York, 2000.
- [31] H. A. Dabkowska, A. B. Dabkowski, R. Hermann, J. Priede, G. Gerbeth, Floating Zone Growth of Oxides and Metallic Alloys Handbook of Crystal Growth. In: P. Rudolph (Ed.), *Handbook of Crystal Growth*, Elsevier, Oxford 2015, pp. 281–329. [doi:10.1016/B978-0-444-63303-3.00008-0](https://doi.org/10.1016/B978-0-444-63303-3.00008-0)